ISSN 1054-660X, Laser Physics, 2009, Vol. 19, No. 1, pp. 129–133.

Design and Alignment Criteria for a Simple, Robust, Diode-Pumped Femtosecond Yb:KYW Oscillator

P. Wasylczyk* and C. Radzewicz

Institute of Experimental Physics, University of Warsaw, ul. Hoza 69, 00-681 Warszawa, Poland

*e-mail: pwasylcz@fuw.edu.pl

Received August 19, 2008; in final form, August 21, 2008

Abstract—We present an efficient, single-diode pumped, prismless Yb:KYW femtosecond laser and study its performance in the soft aperture, Kerr lens mode-locked operation. Practical directions are given to identify the conditions under which high-power, stable mode-locking can be obtained.

PACS numbers: 42.65.Re, 42.55.Xi, 42.60.Fc

DOI: 10.1134/S1054660X0901006X

1. INTRODUCTION

With the Ti:sapphire oscillator being the workhorse in femtosecond-pulse laser applications, the search continues for other designs, preferably diode pumped, that may offer an alternative to the bulky, power-hungry, and expensive green-pumped sources. The choice is limited to materials with absorption bands matching the emission wavelengths of high-power laser diodes as these are developed with other applications in mind. Among the promising dopant atom–pump pairs, the ytterbium–AlGaInAs laser diodes at the 980-nm combination has attracted significant attention in the last few years. New host crystals are presented every now and then—Yb:$KY(WO_4)_2$ (Yb:KYW) [1], Yb:$KGd(WO_4)_2$ (Yb:KGW) [2], Yb:$Sr_3Y(BO_3)_3$ [3], Yb:CaF_2 [4], $CaGdAlO_4$ [5], Yb:Y_2SiO_5 and Yb:Lu_2SiO_5 [6], Yb:YVO_4 [7], as well as Yb:YAG and Yb:glass [8] have all proven to be capable of passive, Kerr-lens mode-locked lasing with the femtosecond pulse generation.

The Yb-doped crystals, glasses, and ceramics are among the potential candidates for compact, reliable femtosecond sources in applications that do not require an ultrabroad spectrum or sub-100 fs pulse durations. A stabilized frequency comb based on an Yb:KYW oscillator has been recently demonstrated [9] and we expect to witness the further development in this and other fields such as femtosecond amplifiers seeding or multiphoton spectroscopy and imaging.

A number of Kerr-lens mode-locked, diode-pumped femtosecond lasers with Yb-doped crystals have been demonstrated—a typical design features an astigmatically compensated X- or Z-fold cavity with a few-millimeters-thick crystal and a prism pair or/and chirped mirror(s) to provide the negative dispersion. A semiconductor saturable absorption mirror (SESAM) is often used to start or/and stabilize the mode-locked operation. The table summarizes a few recent constructions with a variety of host crystals and pump sources, together with their maximum mode-locked powers and the estimated efficiencies reached. The pump power incident on the crystal is given where available.

Two features are visible in the table: a remarkable power scaling with multiwatt powers directly available from femtosecond oscillators with the current diode technology and very high efficiencies reached with single-mode fiber-coupled pump diodes.

In this letter, we present an efficient (33% incident pump-to-output efficiency), simple (single-fiber coupled-diode pumped, no saturable absorber), and robust (prismless) Yb:KYW femtosecond laser. Apart from the laser design and performance analysis, we give practical alignment hints for the stable, Kerr-lens mode-locked operation.

2. THE CRYSTAL

A relatively high thermal conductivity, high nonlinearity (a few times larger than that of Ti:sapphire) [17], low quantum defect resulting in a low thermal load in the laser crystal, and large emission cross sections make Yb:KYW (and, likewise, its twin Yb:KGW) promising candidates for the next generation of femtosecond laser sources. The crystals have been extensively studied in terms of the crystallographic properties, absorption and emission spectra, and thermal conductivity [18–23].

The crystals are now commercially available from several manufacturers with Yb concentrations between 0.5–5.0% (KGW) and 0.5–100.0% (stoichiometric) (KYW) [19].

In our laser, the crystal was 1.2 mm, Brewster cut, KYW doped with Yb at 10 at % (Crystals of Syberia). The pump polarization parallel to the crystal N_m axis and pump propagation along the N_p axis were chosen because of the highest gain [18] and 95% of the incident pump was absorbed in the crystal. Other configurations of the crystal axes are also possible allowing

Yb-doped crystal, passively mode-locked femtosecond lasers with different pump sources. LD—laser diode, MM—multi mode, SM—single mode

Host	Pump source	Pump power, mW	Max. power ML, mW	Efficiency, %	Ref.
KYW	Single emitter LD	2850	120	4	[1]
KYW	Single emitter LD	350	92	26	[10]
KGW	2 single emitter LDs	4000	1100	28	[2]
$Sr_3Y(BO_3)_3$	2 single emitter LDs	2500	300	12	[3]
KYW	Tapered LD	2000	150	8	[11]
KGW	Diode bars	46000	10000	22	[12]
KGW	MM fiber coupled LD	3350	430	13	[13]
KGW	MM fiber coupled LD	6000	150	2.5	[14]
$CaGdAlO_4$	MM fiber coupled LD	4600	38	1	[5]
$Y(Lu)_2SiO_5$	MM fiber coupled LD	15000	2600	17	[6]
CaF_2	MM fiber coupled LD	15000	1400	9	[4]
KYW	SM fiber coupled LD	470	220	47	[15]
YVO_4	SM fiber coupled LD	500	54	11	[7]
KYW	2 SM fiber coupled LDs	970	360	37	[16]
KYW	2 SM fiber coupled LDs	1200	240	20	[9]
KYW	SM fiber coupled LD	521	174	33	This work

different pump wavelengths to be used; the absorption and emission cross sections as well as the spectral widths available should be taken into account while selecting a particular orientation of the crystal.

The crystal was mounted on a copper base with an indium foil for a better thermal contact and the active cooling of the base was provided by a Peltier element. During the experiments, we did not notice any increase in the laser power or a more stable mode-locking with the cooling turned on (base temperature around 10°C; lower temperatures lead to water condensation on the base surfaces); thus, ultimately, the laser was operated with the crystal kept at room temperature.

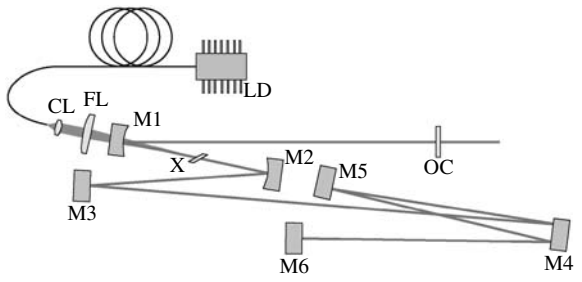

Fig. 1. Femtosecond Yb:KYW oscillator setup. OC—output coupler (2.5 or 5.0% transmission), (M1, M2) $r = -100$ mm pump mirrors, (M3, M5, M6) –250 fs^2 chirped mirrors, plane, (M4) –800 fs^2 chirped mirror, plane, (CL) $f = 15$ mm aspheric collimating lens, (FL) $f = 63$ mm focusing lens, (X) 1.2 mm Yb:KYW crystal, LD—fiber coupled laser diode. The OC arm length is 46 cm (crystal to OC) and the other arm length is 136 cm (crystal to end mirror).

3. THE PUMP

The high efficiency of the longitudinally pumped laser can only be reached with an optimal matching of the pump beam and the laser cavity mode. With the current selection of the commercially available laser diodes, this can be achieved only with the single-mode fiber-coupled single-emitter laser diodes. Reasonable efficiencies have also been reached with single emitter diodes used in a direct, free-space pumping configuration [10], but the possibility of easy pump replacement is limited in such designs. The sources at 980 nm are continuously developed for applications in telecommunications erbium-doped fiber amplifiers (ED FAs) and, throughout the year 2000, their power was increasing by approximately 50% every 18 months. A 750-mW, kink-free module was released in 2007 by Bookham [24], but the central wavelength tolerance is ±5 nm, twice the width of the main absorption peak of the Yb:KYW. In parallel, the uncooled modules are also gaining power, with as much as 300 mW available from a miniature MiniDIL package. All of these devices offer an outstanding reliability, reaching 100 FIT (failures in 10^9 device hours).

The pump source in our design is a SM fiber-coupled laser diode operating at 980 ±0.5 nm (JDSU, 2900 series). The maximum output power of 521 mW (incident on the crystal in the cavity configuration presented in Fig. 1) is reached at a 883-mA drive current. The fiber mode diameter is 4 μm and the fiber output beam is first collimated with an aspheric lens collimator with a 15-mm focal length (glass, AR coated for near IR, Thorlabs) and subsequently focused onto the laser

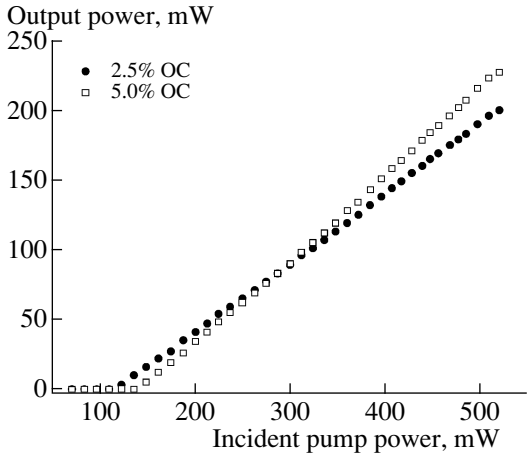

Fig. 2. Laser output power versus the pump power incident on the crystal for two output couplers: 2.5% transmission (solid circles) and 5.0% transmission (open squares).

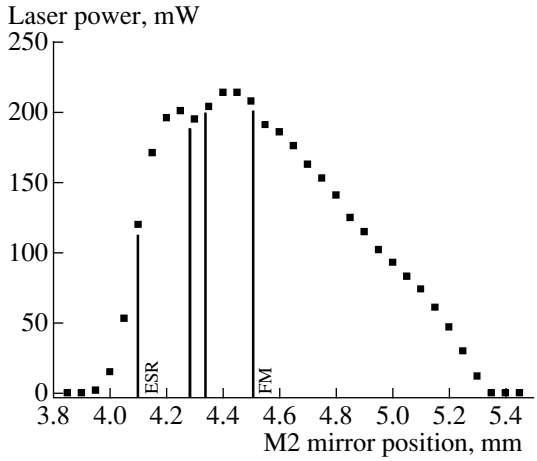

Fig. 3. Measured CW output power as a function of the concave mirror (M2) position (arbitrary zero on the horizontal scale). The vertical lines indicate the four regions where mode-locking is obtained with two of them exhibiting characteristic mode shapes—near the inner edge of the stability region (ESR) and at the "fish mode" (FM).

crystal by a 63-mm-focal length planoconcave singlet (fused silica, uncoated) to a measured beam diameter of 17 μm. The fiber is terminated with a standard FC connector, which is essential for easy pump replacement. Indeed, when the connector was disconnected and then connected again, the laser required only a minor correction to return to the highest power level and we believe that, with a sufficiently stable mechanics, the pump diode may be field replaceable. We did not used a half-waveplate to control the pump beam polarization direction. Instead, the fiber collimator was mounted in such a way that it can be rotated around the beam axis and the pump polarization is adjusted to minimize the Brewster reflection from the crystal surface. Although the diode fiber is polarization maintaining, the pump beam emerging from the focusing optics is not perfectly polarized and an additional cube polarizer makes this alignment stage easier.

The diode 14-pin butterfly package has a built-in Peltier element that provides cooling and temperature stabilization at 20°C (ambient) when supplied with a 0.46-A current at the maximum diode power.

4. DISPERSION CONTROL

All solid-state, Yb-doped crystal, passively mode-locked femtosecond lasers demonstrated until now operated in the regime of a large negative dispersion. This is achieved by inserting a prism pair in the cavity, using chirped mirrors or both [6, 9]. In our design, the negative dispersion is provided by a set of four mirrors with a negative group velocity dispersion (Layertec) resulting in a net dispersion (chirped mirrors + crystal) of around -3970 fs^2 per cavity roundtrip in the spectral region of 1040 ± 20 nm.

The design of the chirped pump mirrors is challenging due to the small difference between the pump and laser wavelengths. The dispersion of the pump mirrors in our laser was not specified. The output couplers have a negligible GVD of below 20 fs^2.

With the pump diode installed on a custom-made PCB with a quick release mount (Azimuth Electronics), the overall footprint of the laser head does not exceed 20×70 cm.

5. CW OPERATION

The laser was first aligned and operated in the CW regime. Two output couplers were tested and both provided a similar performance in CW as well as in mode-locked operation. The slope efficiency was 50% (61%) with a 2.5% (5.0%) transmission OC. The output power versus the pump power (measured in front of the crystal) is presented in Fig. 2.

The CW output power was also measured as a function of the mirror M2 position (Fig. 3, compare to a similar measurement for the high repetition rate, three-element cavity in [15]). The laser cavity has a stability region spanning more than a millimeter with a steep inner edge and a more gradual outer edge. The position of this steep inner edge is a characteristic marking point that allows us to identify potential regions where the Kerr lens mode-locking may be expected, as described below. While analyzing the plot in Fig. 3, one should keep in mind that such a large translation of the concave mirror may result in the cavity misalignment unless the laser mode axis is perfectly parallel to the translation direction.

6. MODE-LOCKING

Even with the simple configuration presented, without SESAM, the laser mode-locks easily after a small,

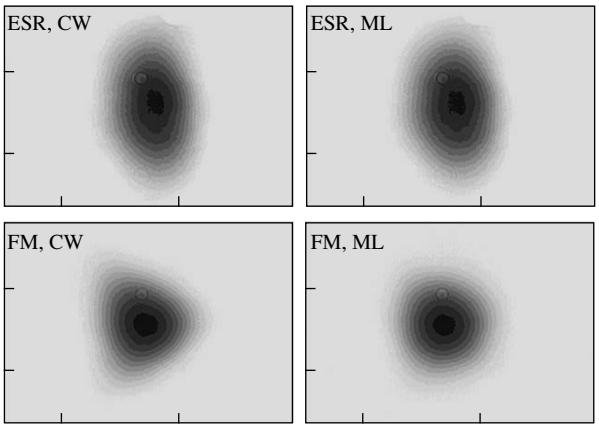

Fig. 4. Measured beam shapes in the CW and mode-locked regimes of operation for two regions: ESR and FM. Logarithmic scales of grey with black corresponding to the highest intensity.

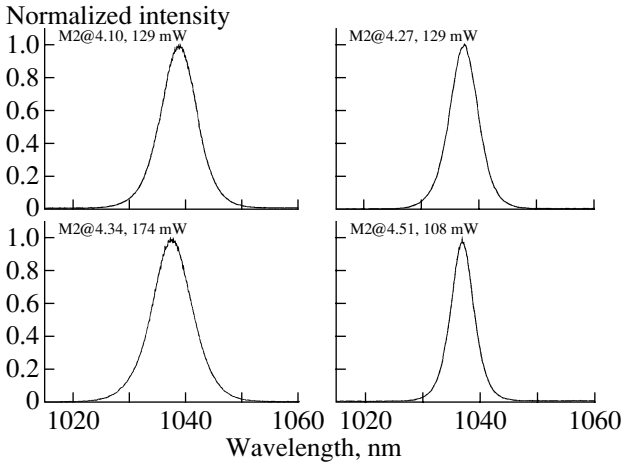

Fig. 5. Measured laser spectra for four mode-locking regions labeled by the M2 mirror position (compare Fig. 3) and the maximum mode-locked output powers.

fast translation of mirror M2 towards the crystal within the four regions of the mirror M2 position, as indicated in Fig. 3. Stable mode-locking is maintained for several hours, even though no special care was taken to design an ultrastable mechanics or to seal the cavity in a box.

Apart from the position within the stability region of the laser cavity (which may be challenging to measure with a high precision), the far-field laser beam shape proves to be an useful criterion for the mode-locked laser alignment. Once the cavity is aligned in the CW mode, a characteristic behavior can be observed as the concave mirror M2 is translated. The beam profiles recorded with a CCD camera positioned around 50 cm from the output coupler are presented in Fig. 4 for the two, easily identifiable cases. In the vicinity of the inner edge of the stability region, the mode becomes elliptical with the longer axis vertical and, eventually, disappears as mirror M2 is moved towards the crystal. A different behavior—the beam disappears without being stretched vertically or falls apart into many separate beams—indicates a poor cavity alignment. The inner edge of the outer stability region (ESR) is often chosen for soft-aperture Kerr-lens mode-locking since it provides a high increase in the pump–cavity mode overlap compared to the CW regime and, thus, a stable pulsing can be obtained [25].

Another characteristic region is the so-called "fish mode" (FM), where the beam becomes triangular and minute changes in the M2 mirror position lead to switching between two mode shapes, both triangular but flipped in the horizontal direction. This region can provide output powers much higher than those in the ESR region.

In both ERS and FM regions, the transition from the CW to mode-locked operation is accompanied by a change in the beam shape which becomes closer to the symmetric, circular Gaussian.

In our Yb:KYW oscillator, we have also identified two other regions where stable mode-locking was observed, which do not exhibit any characteristic beam profiles and lay between the ESR and FM positions as presented in Fig. 3. All four regions of the mode-locked operation are quite narrow and precise positioning of M2 is essential.

The laser spectra measured in all of the mode-locking configurations are presented in Fig. 5. The spectra are centered in the vicinity of 1037 nm and their width (FWHM) varies from 4 (M2@4.51) to 8 nm (M2@4.34) with the spectral wings spanning the 1020–1055-nm range in the latter configuration.

The maximum mode-locked output power achieved was 174 mW, which corresponds to 33% of the incident pump-optical output efficiency. This was reached in the third (closer to the FM) region. In this configuration, the measured background-free autocorrelation had a FWHM of 315 fs at a pulse repetition rate of 82 MHz.

In the "fish mode" region, the CW power was the highest of the four regions found, but, in the mode-locked regime, the pump power had to be significantly decreased to suppress the CW spike in the laser spectrum. As a result, the ML power in the FM was below 110 mW and could not be increased with a higher transmission OC.

7. CONCLUSIONS

We have provided the design and alignment criteria for a simple, diode-pumped Yb:KYW femtosecond laser. In the *Z*-shaped laser cavity, we have identified four separate regions in which the Kerr lens mode-locking is easily initiated by a small mechanical disturbance. The good overlap between the pump beam and the laser cavity mode resulted in an efficiency of 33%. With the increasing power and falling prices of the sin-

gle-mode fiber-coupled diodes available to pump Yb-doped materials, the next generation of ultrashort pulse sources will offer unprecedented compactness (comparable with that of the fiber lasers and, potentially, with a significantly higher power) and, for the first time, may become available to a number of demanding applications outside research laboratories.

ACKNOWLEDGMENTS

This work has been supported financially by the Polish Government (MNiSW grant no. R02 043 02). P.W. gratefully acknowledges the generous support of the Foundation for Polish Science funded through a grant from Iceland, Liechtenstein, and Norway through the EEA Financial Mechanism.

REFERENCES

1. H. Liu, J. Nees, and G. Mourou, Opt. Lett. **26**, 1723 (2001).
2. F. Brunner, G. J. Sphler, J. Aus der Au, et al., Opt. Lett. **25**, 1119 (2000).
3. F. Druon, S. Chnais, P. Raybaut, et al., Opt. Lett. **27**, 197 (2002).
4. A. Lucca, G. Debourg, M. Jacquemet, et al., Opt. Lett. **29**, 2767 (2004).
5. Y. Zaouter, J. Didierjean, F. Balembois, et al., Opt. Lett. **31**, 119 (2006).
6. F. Thibault, D. Pelenc, F. Druon, et al., Opt. Lett. **31**, 1555 (2006).
7. A. A. Lagatsky, A. R. Sarmani, C. T. A. Brown, et al., Opt. Lett. **30**, 3234 (2005).
8. C. Honninger, R. Paschotta, M. Graf, et al., Appl. Phys. B **69**, 3 (1999).
9. S. A. Meyer, J. A. Squier, and S. A. Diddams, Eur. Phys. J. D **48**, 19 (2008).
10. A. R. Sarmani, A. A. Lagatsky, C. T. A. Brown, and W. Sibbett, in *Proc. of the Conference on Lasers and Electro-Optics Europe, June 2005* (2005), p. 18.
11. P. Klopp, V. Petrov, U. Griebner, and G. Erbert, Opt. Expr. **10**, 108 (2002).
12. G. R. Holtom, Opt. Lett. **31**, 2719 (2006).
13. G. Paunescu, J. Hein, and R. Sauerbrey, Appl. Phys. B **79**, 555 (2004).
14. A. Major, V. Barzda, P. A. E. Piunno, et al., Opt. Expr. **14**, 5285 (2006).
15. A. A. Lagatsky, C. T. A. Brown, and W. Sibbett, Opt. Expr. **12**, 3928 (2004).
16. A. A. Lagatsky, E. U. Rafailov, A. R. Sarmani, et al., Opt. Lett. **30**, 1144 (2005).
17. A. Major, I. Nikolakakos, J. S. Aitchison, et al., Appl. Phys. B **77**, 433 (2003).
18. N. V. Kuleshov, A. A. Lagatsky, A. V. Podlipensky, et al., Opt. Lett. **22**, 1317 (1997).
19. M. C. Pujol, M. A. Bursukova, F. Guell, et al., Phys. Rev. B **65**, 165121 (2002).
20. C. Pujol, M. Aguil, F. Daz, and C. Zaldo, Opt. Mat. **13**, 33–40 (1999).
21. G. Métrat, M. Boudeulle, N. Muhlstein, et al., J. Cryst. Growth **197**, 883 (1999).
22. N. V. Kuleshov, A. A. Lagatsky, V. G. Shcherbitsky, et al., Appl. Phys. B **64**, 409 (1997).
23. A. A. Demidovich, A. N. Kuzminb, N. K. Nikeenko, et al., J. Alloys Comp. **341**, 124 (2002).
24. www.bookham.com.
25. V. Magni, G. Cerullo, and S. DeSilvestri, Opt. Comm. **101**, 365 (1993).